

Supporting Information

Purdon et al. 10.1073/pnas.1221180110

SI Materials and Methods

To analyze low-frequency phase modulation across a wider range of high frequencies, we also computed phase-triggered spectrograms. We used the low-frequency phase $\psi(t)$ to find the low-frequency oscillation peaks, [i.e., $\psi(t) = 0$], and computed the spectrogram within time windows of ± 2 s of these peaks. Within each 10-min epoch, we computed the spectrogram with different time-frequency parameters that would provide greater temporal resolution to quantify power across different phases of the slow oscillation (window length $T = 4$ s, time-bandwidth product $TW = 1$, number of tapers $K = 1$, no overlap, spectral resolution 0.5 Hz). We computed the median spectrogram over all 4-s windows within a 2-min epoch. We then normalized the spectrogram for

each subject at each frequency by the mean over all time lags (± 2 s), normalizing for the average power in each frequency bin. We performed this calculation over a 2-min period centered at the loss of consciousness (LOC) time point to characterize the trough-max modulation pattern and also over a 2-min period centered 30 min beyond LOC to characterize the peak-maximum modulation pattern. Fig. S3 shows the phase-triggered spectrograms, averaged across subjects, and the corresponding average low-frequency waveform. These results show that the low-frequency oscillation modulates a broad range of higher frequencies spanning theta through gamma bands, in both the trough-max and peak-max regimes.

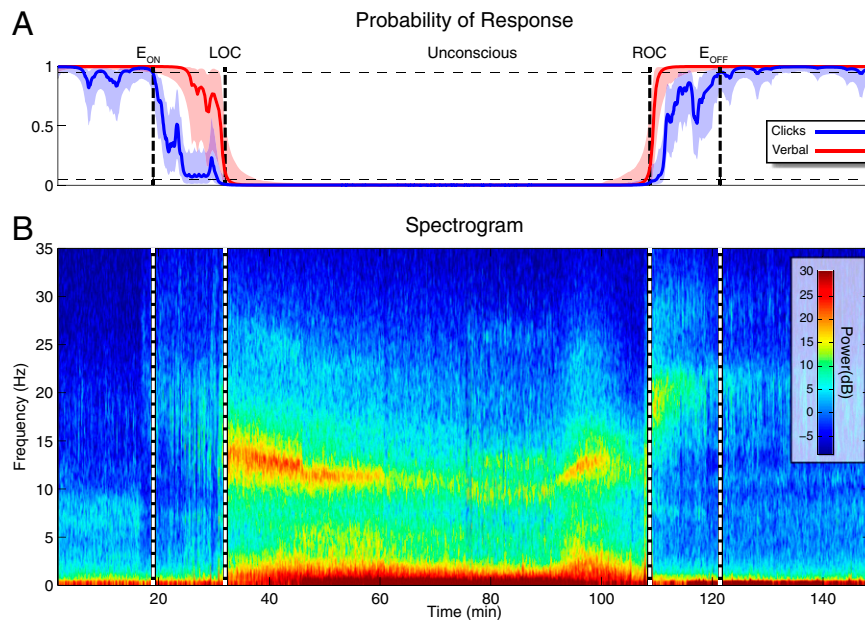


Fig. S1. Example of individual subject behavior and spectrogram. (A) The response-probability curves show a significant difference between verbal and click stimuli and allow us to construct behaviorally defined markers for the onset (E_{ON}) and offset (E_{OFF}) of drug effects as well as loss of consciousness (LOC) and recovery of consciousness (ROC). (B) The changes in gamma, beta, alpha, and slow oscillation power observed in Fig. 2, the appearance of a traveling peak as in Fig. 3, and their timing relative to behavior can be seen readily within the individual subject spectrogram.

Spatial Distribution of Power in Frequency Bands

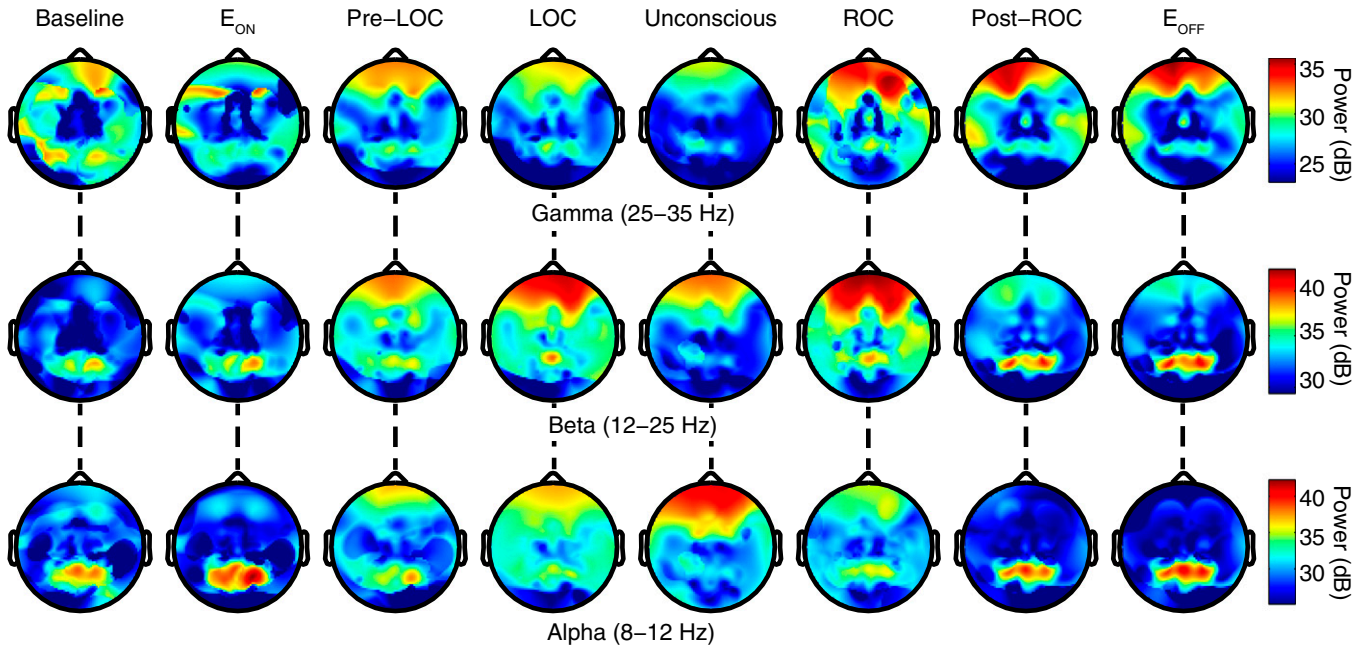


Fig. S2. Spatial distribution of power in the gamma, beta, and alpha bands at different behavioral end points. These results show how power within the traveling peak is reflected in the spatial distribution within these traditional frequency bands.

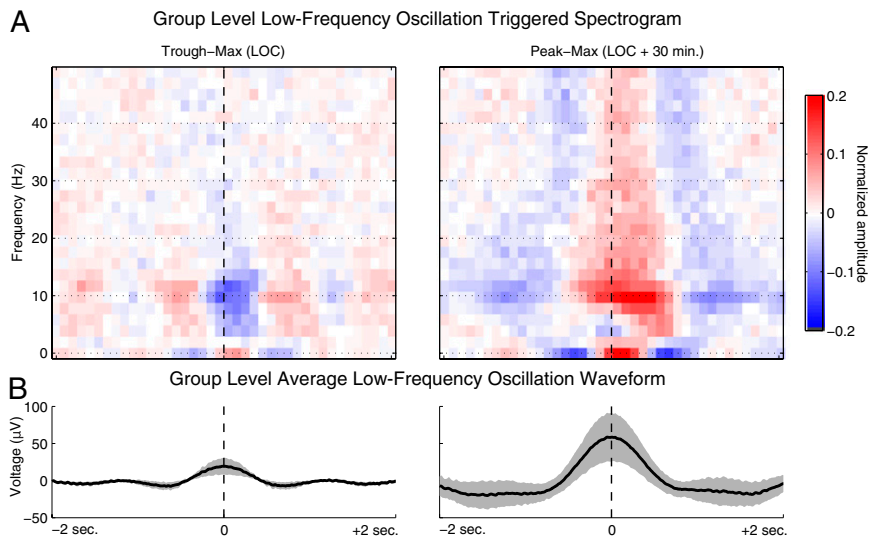


Fig. S3. The low-frequency (0.1–1 Hz) phase modulates a range of higher frequencies. (A) Cross-subject average EEG spectrogram triggered at peaks of low-frequency oscillations at LOC (Left) and 30 min later (Right). Power at each frequency is normalized by the mean power across time at that frequency. (B) Average peak-triggered low-frequency waveform, with SEs (gray shading), at LOC (Left) and 30 min later (Right). These results show that the low-frequency oscillation modulates a broad range of higher frequencies spanning theta through gamma bands in both the trough-max and peak-max regimes.